

Wavelet Estimation for Factor Models with Time-Varying Loadings

Duván Humberto Cataño^{*,†},
C. Vladimir Rodríguez-Caballero[‡],
Chang Chiann[§],
Daniel Peña[¶]

Abstract

We introduce a high-dimensional factor model with time-varying loadings. We cover both stationary and nonstationary factors to increase the possibilities of applications. We propose an estimation procedure based on two stages. First, we estimate common factors by principal components. In the second step, considering the estimated factors as observed, the time-varying loadings are estimated by an iterative generalized least squares procedure using wavelet functions. We investigate the finite sample features by some Monte Carlo simulations. Finally, we apply the model to study the Nord Pool power market's electricity prices and loads.

Keywords: Factor models, wavelet functions, generalized least squares, electricity prices and loads.

1 Introduction

Factor models have been widely used in the last decade due to their ability to explain the structure of a common variability among time series by a small number of unobservable common factors. In this sense, these models are used to reduce the dimensionality of complex systems. The studies of factor models have encompassed the stationary and nonstationary frameworks by different estimation methods, see

^{*}The author would like to thank financial supports from CAPES, CNPq, and University of Sao Paulo, Brazil.

[†]University of Antioquia, Colombia.

[‡]Corresponding author. Department of Statistics, ITAM, Mexico & CREATES, Aarhus University, Denmark. Address: Río Hondo No.1, Col. Progreso Tizapán, Álvaro Obregón, CDMX. 01080. Mexico. E-mail: vladimir.rodriguez@itam.mx

[§]University of Sao Paulo, IME, São Paulo, Brasil

[¶]Department of Statistics and Institute UC3M-BS of Financial Big Data. Universidad Carlos III de Madrid, Getafe, Spain.

among many others, [Peña and Box \(1987\)](#), [Forni et al. \(2000\)](#), [Stock and Watson \(2002\)](#), [Bai and Ng \(2002\)](#), [Bai \(2003\)](#), [Forni et al. \(2004\)](#), [Forni et al. \(2005\)](#), [Lam et al. \(2012\)](#), [Bai and Li \(2016\)](#), [Chan et al. \(2017\)](#), and [Gao and Tsay \(2019\)](#) for stationary cases, and [Bai and Ng \(2004\)](#), [Peña and Poncela \(2006\)](#), [Barigozzi et al. \(2016\)](#), and [Rodríguez-Caballero and Ergemen \(2017\)](#) for nonstationary cases.

The literature has recently focused on a particular framework of factor models that allow the loadings to vary over time. [Motta et al. \(2011\)](#) introduce deterministic smooth variations in factor loadings and propose estimation procedures based on locally weighted generalized least squares using kernel functions under a time-domain approach. Similarly, [Eichler et al. \(2011\)](#) allow for a nonstationary structure in the factor model with deterministic time-dependent functions in factor loadings. Their estimation procedure can be seen as a time-varying spectral density matrix of the underlying process. Furthermore, [Mikkelsen et al. \(2018\)](#) propose a factor model with time-varying loadings that evolve as stationary VAR processes employing Kalman filter procedures to obtain the maximum likelihood estimators of the factor loadings parameters.

In this paper, we use wavelet functions to define smooth variations of loadings in high-dimensional factor models. Our model can be helpful in some economic applications when the dynamics are driven by smooth variations, whose cumulative effects cannot be ignored, see [Su and Wang \(2017\)](#), and [Bai and Han \(2016\)](#), for details. In our framework, to capture the common smooth variations in the vector of time series, parameters in the loading matrix are assumed to be well approximated by deterministic functions over time.

The estimation procedure consists of two steps. First, following [Mikkelsen et al. \(2018\)](#), common factors are estimated by principal component analysis (PCA). In the second step, using estimated factors of the first stage, factor loadings are estimated by an iterative procedure that combines generalized least squares (GLS) using wavelet functions. We show that factors estimated by principal components are consistent after controlling the magnitude of the loadings' instabilities. We highlight that a requirement for such consistency is that common factors need to be independent of factor loadings' functions. We also study the case of nonstationary factors following the approach of [Peña and Poncela \(2006\)](#), who propose to use a generalized covariance matrix to estimate common factors.

We use Monte Carlo simulations to show that the method correctly identifies the factors and loadings even in relatively small samples. Finally, we use the methodology proposed to analyze the Nord Pool power market. We use the electricity system prices and loads throughout two years and a half to show that factor loadings are not invariant along time, illustrating our model's usefulness. We find that some features of electricity prices and loads, see, e.g., [Weron \(2007\)](#), and [Weron \(2014\)](#), are well extracted by common factors estimates and by time-varying loadings estimates.

In short, the contributions of this article are i) We propose wavelet functions to estimate time-varying loadings and a consistent method to estimate them; ii) we also allow for nonstationary factors to cover more possibilities of application, and

iii) the usefulness of the model is discussed through a Monte Carlo study, and by the empirical application.

The remainder of the paper is organized as follows. Section 2 introduces the model, shows the consistency of principal components with stationary and nonstationary variables, and introduces the wavelet functions. Section 3 discusses the estimation procedure. Monte Carlo experiments are presented in Section 4, whereas an empirical illustration is provided in Section 5. Finally, Section 6 concludes. We use bold-unslanted letters for matrices, bold-slanted letters for vectors, and unbold letters for scalars. We denote by $tr(\cdot)$ the trace operator, by $rank(\mathbf{A})$ the rank of a matrix \mathbf{A} , by \mathbb{I}_n the identity matrix of dimension n , by \otimes the Kronecker product and by $\|\cdot\|$ the Frobenius (Euclidean) norm, i.e., $\|\mathbf{A}\| = \sqrt{tr(\mathbf{A}'\mathbf{A})}$.

2 The model

In this section, we introduce the model. First, we consider stationary factors to motivate the general setup and the estimation procedure. Then, in the next section, we relax the stationarity assumption to allow for nonstationary factors.

2.1 Stationary factors

The model we propose is as follows

$$\mathbf{Y}_t = \mathbf{X}_t + \mathbf{e}_t, \quad (1)$$

$$\mathbf{X}_t = [\mathbf{\Lambda}_0 + \mathbf{\Lambda}(t/T)]\mathbf{F}_t, \quad (2)$$

where the common component, \mathbf{X}_t , is an N -dimensional locally stationary process, in the sense of [Dahlhaus et al. \(1997b\)](#), and the loadings are defined in the re-scaled time, $u = t/T \in [0, 1]$. \mathbf{F}_t are the unobservable common factors and \mathbf{e}_t , the idiosyncratic component, is a sequence of weakly dependent variables, see e.g. [Stock and Watson \(2002\)](#), and [Bai \(2003\)](#).

$\mathbf{\Lambda}(u) = \{\lambda_{ij}(u), i = 1, \dots, N; j = 1, \dots, r\}$, is the time-dependent factor loading matrix. In this respect, the influence of \mathbf{F}_t on the observed process varies over time, and $\mathbf{\Lambda}(u)$ captures the smooth variations of the loadings with respect $\mathbf{\Lambda}_0$, a constant loading matrix.

When $\mathbf{\Lambda}(u) = 0, \forall u \in [0, 1]$, the standard factor model is considered; therefore, the model proposed in (1) can be seen as a generalization of the standard factor model of [Bai \(2003\)](#).

Definition 1. *The sequence \mathbf{Y}_t in (1) follows a factor model with time-varying loadings if:*

- a. For $N \in \mathbb{N}$, there is a function with

$$\begin{aligned} \mathbf{\Lambda}(\cdot) &: [0, 1] \rightarrow \mathbb{R}^{N \times r} \\ u &\mapsto \mathbf{\Lambda}(u), \end{aligned}$$

such that $\forall T \in \mathbb{N}$,

$$\Gamma_Y(u) = [\mathbf{\Lambda}_0 + \mathbf{\Lambda}(u)]\Gamma_F[\mathbf{\Lambda}_0 + \mathbf{\Lambda}(u)]' + \Gamma_e,$$

with $\text{rank}[\mathbf{\Lambda}_0 + \mathbf{\Lambda}(u)] = r$, and $\Gamma_F = \mathbb{V}\text{ar}(\mathbf{F}_t)$ is a positive definite diagonal matrix.

b. $\Gamma_e = \text{var}(\mathbf{e}_t)$ is a positive definite matrix.

With an arbitrary constant $Q \in \mathbb{R}^+$, we then use the following assumptions to study the model in (1) following [Bai and Ng \(2002\)](#).

Assumption A. Factors:

$$A_1 \quad \mathbb{E}\|\mathbf{F}_t\|^4 < Q,$$

$$A_2 \quad T^{-1} \sum_{t=1}^T \mathbf{F}_t \mathbf{F}_t' \xrightarrow{p} \Gamma_F \text{ as } T \rightarrow \infty, \text{ with } \Gamma_F \text{ is a positive definite diagonal matrix.}$$

Assumption B. Factor loadings:

$$B_1 \quad \|\boldsymbol{\lambda}_{i0}\| \leq \bar{\lambda} \text{ and } \|\mathbf{\Lambda}_0' \mathbf{\Lambda}_0 / N - D\| \rightarrow 0, \text{ as } N \rightarrow \infty, \text{ with } r \times r \text{ positive definite matrix } D, \text{ and } \boldsymbol{\lambda}_{i0} \text{ is the } i\text{-th row of } \mathbf{\Lambda}_0,$$

$$B_2 \quad \sup_{u \in (0,1)} \|\boldsymbol{\lambda}_i(u)\| \leq \bar{\lambda} < \infty, \text{ where } \boldsymbol{\lambda}_i(u) \text{ is the } i\text{-th row of } \mathbf{\Lambda}(u),$$

$$B_3 \quad \lambda_{ij}(u) \in L^2[0,1], \quad \text{for } i = 1, \dots, N \text{ and } j = 1, \dots, r.$$

Assumption C. Idiosyncratic terms:

$$C_1 \quad \mathbb{E}(e_{it}) = 0, \mathbb{E}|e_{it}|^4 < Q,$$

$$C_2 \quad \mathbb{E}[e_{it}e_{jt}] = \tau_{ij,t}, \text{ with } |\tau_{ij,t}| < |\tau_{ij}|, \text{ for a constant } |\tau_{ij}| \text{ and } N^{-1} \sum_{i,j=1}^N |\tau_{ij}| < Q, \forall t,$$

$$C_3 \quad \mathbb{E}[N^{-1} \sum_{i=1}^N e_{is}e_{it}] = \gamma_N(s, t), |\gamma_N(s, s)| < Q, \forall (s, t); \text{ and } T^{-1} \sum_{s=1}^T \sum_{t=1}^T |\gamma_N(s, t)| < Q.$$

Assumption D. Time-varying factor loadings and factors:

K_{1NT} , K_{2NT} and K_{3NT} are functions such that the following conditions are fulfilled for any $n, m, k, q = 1, \dots, r$ and $\lambda_{ij}(s/T) \equiv \lambda_{ij}(s)$.

$$D_1 \quad \sup_{s,t} \sum_{i,j}^N |\lambda_{in}(s)\lambda_{jm}(t)| |\mathbb{E}[F_{ns}F_{mt}]| < K_{1NT},$$

$$D_2 \quad \sum_{s,t=1}^T \sum_{i,j=1}^N |\lambda_{in}(s)\lambda_{jm}(s)| |\mathbb{E}[F_{ns}F_{ms}F_{kt}F_{qt}]| < K_{2NT},$$

$$D_3 \quad \sup_{s,t} \sum_{s=1}^T \sum_{i,j=1}^N |\lambda_{in}(s)\lambda_{jm}(s)\lambda_{ik}(t)\lambda_{jq}(t)| |\mathbb{E}[F_{ns}F_{ms}F_{kt}F_{qt}]| < K_{3NT}.$$

Assumption E. Independence:

The process e_{it} and F_{js} are independent of each other for any (i, j, s, t) .

Assumption A imposes standard moment conditions. The unobservable factors have finite fourth moments, and their covariance converges in probability to a positive definite matrix. Assumptions B_1 and B_2 ensure that each factor has a nontrivial contribution to the variance of \mathbf{Y}_t . Assumption B_3 ensures the existence of the expansion in the wavelet function for the factor loadings. Assumption C allows dependence in the idiosyncratic process. Assumption D is required to guarantee the consistency of the principal components. Finally, independence between factors and the idiosyncratic term is provided in Assumption E.

2.1.1 Principal component estimators

We use PCA to estimate the factors \mathbf{F}_t . It is well-known that principal components are obtained solving the optimization problem

$$\min_{\mathbf{F}, \mathbf{\Lambda}} (NT)^{-1} \sum_{i=1}^N \sum_{t=1}^T (Y_{it} - \lambda'_i \mathbf{F}_t)^2, \quad (3)$$

where $\mathbf{F} = (\mathbf{F}_1, \mathbf{F}_2, \dots, \mathbf{F}_T)'$ is a $T \times r$ matrix and $\mathbf{\Lambda}$ is a $N \times r$ matrix. We need to impose some restrictions to guarantee the identification of the parameters. Solving for $\mathbf{\Lambda}$, the normalization $\mathbf{F}'\mathbf{F} = \mathbb{I}_r$ provides the necessary number of restrictions.

With this, minimize (3) is equivalent to maximize $tr[\mathbf{F}'(\mathbf{Y}\mathbf{Y}')\mathbf{F}]$, where $\mathbf{Y} = (\mathbf{Y}_1, \dots, \mathbf{Y}_T)'$. Then, the estimated factor matrix, $\tilde{\mathbf{F}}$, is \sqrt{T} times the eigenvectors corresponding to the r largest eigenvalues of the $T \times T$ matrix $\mathbf{Y}\mathbf{Y}'$. It is well-known that this solution is not unique, that is, any orthogonal rotation of $\tilde{\mathbf{F}}$ is also a solution. See [Bai et al. \(2008\)](#) for more details.

The following theorem is a modified version of Theorem 1 in [Bates et al. \(2013\)](#) and shows that, under the assumptions previously stated, it is possible to consistently estimate any rotation of the factors by principal components even if the loadings are time-varying.

Theorem 1. *Under Assumptions A-E, there exists an $r \times r$ matrix H , such that*

$$T^{-1} \sum_{t=1}^T \|\tilde{\mathbf{F}}_t - H' \mathbf{F}_t\|^2 = O_p(R_{NT}), \quad (4)$$

as $N, T \rightarrow \infty$, where $R_{NT} = \max \left\{ \frac{1}{N}, \frac{1}{NT}, \frac{K_{1NT}}{N^2}, \frac{K_{2NT}}{N^2 T^2}, \frac{K_{3NT}}{N^2 T^2} \right\}$ with K_{1NT} , K_{2NT} , and K_{3NT} defined in the Assumption D. Furthermore,

$$H = (\mathbf{\Lambda}'_0 \mathbf{\Lambda}_0 / N) (\mathbf{F}' \tilde{\mathbf{F}} / T) V_{NT}^{-1},$$

where V_{NT} is a diagonal matrix of the r largest eigenvalues of the matrix $(NT)^{-1} \mathbf{Y}\mathbf{Y}'$.

Proof. See the appendix A.1.

Theorem 1 points out that the average squared deviation between the estimated factors and the space spanned by a rotation of the actual factors will vanish

at rate R_{NT} , which is similar to that in [Bai and Ng \(2002\)](#). Note that from (4), the estimated common factors, $\tilde{\mathbf{F}}_t$, are identified through a rotation, then, principal components converge to a rotation of the actual common factors $H'\mathbf{F}_t$.

2.2 The nonstationary model

In many areas, as in economics and finances, finding strong evidence of nonstationary processes has repeatedly been reported in many empirical studies. Consequently, it is natural to think that many panel data may include nonstationary economic or financial variables. There has been some debate concerning the use of differenced variables. The main argument being discussed is whether differencing the series causes a severe loss of information.

In this section, we allow for nonstationary variables in model 1. Then, assume that Y_t is $I(d)$. Note that while assumptions B-E do not differ under the nonstationary setup, we should modify the factor structure's assumption. With this in mind, we follow the assumption 1 in [Peña and Poncela \(2006\)](#) to define the r_1 nonstationary common factors as follows

Assumption F. Nonstationary Factors:

$$(1 - L)^d \mathbf{f}_{1,t} = \mu + \mathbf{u}_t, \\ \mathbf{u}_t = \Psi(L)\mathbf{a}_{1,t},$$

where L is the lag operator, d is a positive integer, μ is a $r_1 \times 1$ vector of drifts, $E(\mathbf{a}_{1,t}) = \mathbf{0}$, $\text{var}(\mathbf{a}_{1,t}) = \Sigma_1 > 0$, $\mathbf{f}_{1,-(d-1)} = \mathbf{f}_{1,-(d-2)} = \dots = \mathbf{f}_{1,0} = \mathbf{0}$, $\sum_i \|\Psi_i\| < \infty$ and $\|\mathbf{M}\| = [\text{tr}(\mathbf{M}'\mathbf{M})]^{1/2}$ for any matrix or vector M . Define $\Psi(1) = \sum_{i=0}^{\infty} \Psi_i$ with $\text{rank}(\Psi(1)) = r_1$.

To estimate the nonstationary model, we use the methodology proposed by [Peña and Poncela \(2006\)](#), who use generalized covariance matrices defined as

$$\mathbf{C}_y(k) = \frac{1}{T^{2d+d'}} \sum_{t=k+1}^T (\mathbf{Y}_{t-k} - \bar{\mathbf{Y}}_t)(\mathbf{Y}_t - \bar{\mathbf{Y}}_t), \quad (5)$$

where $\bar{\mathbf{Y}} = \frac{1}{T} \sum_{t=1}^T \mathbf{Y}_t$ and d' can be either 0 or 1.

Under this framework, consistent factor estimates are given by

$$\hat{\mathbf{F}} = \mathbf{Y} \hat{\mathbf{\Lambda}}, \quad (6)$$

where $\hat{\mathbf{F}} = (\hat{\mathbf{F}}_1, \hat{\mathbf{F}}_2, \dots, \hat{\mathbf{F}}_T)'$ is a $T \times r$ matrix, $\mathbf{Y} = (\mathbf{Y}_1, \dots, \mathbf{Y}_T)'$ is a $T \times N$ matrix and $\hat{\mathbf{\Lambda}}$ is a $N \times r$ matrix composed by the first r eigenvectors of $\mathbf{C}_y(k)$. Following the same reasoning as in Theorem 1, it can be shown that the average squared deviation between the estimated factors (6) and space spanned by a rotation of the actual factors will vanish as $(N, T) \rightarrow \infty$.

2.3 Wavelets

The basic idea of a wavelet is to construct infinite collections of translated and scaled versions of the scaling function $\phi(t)$ and the wavelet $\psi(t)$ such as $\phi_{jk}(t) = 2^{j/2}\phi(2^j t - k)$, and $\psi_{jk}(t) = 2^{j/2}\psi(2^j t - k)$ for $j, k \in \mathbb{Z}$. Suppose that $\{\phi_{lk}(\cdot)\}_{k \in \mathbb{Z}} \cup \{\psi_{jk}(\cdot)\}_{j \geq l; k \in \mathbb{Z}}$ forms an orthonormal basis of $L^2(\mathbb{R})$, for any coarse scale l . A key point is to construct ϕ and ψ with a compact support that generates an orthonormal system, which has location in time-frequency. From this, we can get parsimonious representations for a wide class of wavelet functions, further details in [Chiann and Morettin \(2005\)](#), and [Porto et al. \(2008\)](#).

In some applications, these functions are defined in a compact set in $[0, 1]$ for functions $\lambda_{ij}(u)$, for $i = 1, \dots, N$ and $j = 1, \dots, r$ defined in (2). Then, it is necessary to consider an orthonormal system that generates $L^2[0, 1]$. For the construction of these orthonormal systems, we follow the procedure by [Cohen and Ryan \(1995\)](#), that generates multiresolution levels $\tilde{V}_0 \subset \tilde{V}_1 \subset \dots$, where the spaces \tilde{V}_j are generated by $\tilde{\psi}_{jk}$. Negative values of j are not necessary since $\tilde{\phi} = \tilde{\phi}_{00} = 1$, and if $j \leq 0$, $\tilde{\psi}_{jk}(u) = 2^{-j/2}$, see [Vidakovic \(2009\)](#) for more details and different approaches. Therefore, for any function $\lambda(u) \in L^2[0, 1]$, can be expand in series of orthogonal functions

$$\lambda(u) = \alpha_{00}\phi(u) + \sum_{j \geq 0} \sum_{k \in I_j} \beta_{jk}\psi_{jk}(u), \quad (7)$$

where we take $l = 0$ and $I_j = \{k : k = 0, \dots, 2^j - 1\}$. For each j , the set I_j generates values of k such that β_{jk} belongs to the scale 2^j . For example, for $j = 3$, there are eight wavelet coefficients in the scale 2^3 , whereas for $j = 2$, only four coefficients in the scale 2^2 .

Some applications consider the equation in (7) for a maximum resolution level J , through

$$\lambda(u) \approx \alpha_{00}\phi(u) + \sum_{j=0}^{J-1} \sum_{k \in I_j} \beta_{jk}\psi_{jk}(u). \quad (8)$$

In this way, the function $\lambda(u)$ approximates to the space \tilde{V}_J . We use ordinary wavelets as in [Dahlhaus et al. \(1997a\)](#) because the performance is suitable in the case of smooth functions. Particularly, we employ Daubechies ($D8$, hereafter) and Haar wavelets of compact supports.

3 Estimation of time-varying loadings by wavelets

We consider the process in (1) with r common factors ($r < N$) to discuss the estimation procedure of the time-varying loadings. From now on, we consider the loading matrix, $[\Lambda(u) + \Lambda_0]$, as a unique function over time $\Lambda(u)$, given by

$$\mathbf{Y}_t = \Lambda(u)\mathbf{F}_t + \mathbf{e}_t, \quad (9)$$

with $t = 1, 2, \dots, T$, and $u = t/T \in [0, 1]$. In matrix form, we have

$$\begin{bmatrix} Y_{1t} \\ Y_{2t} \\ \vdots \\ Y_{rt} \\ \vdots \\ Y_{Nt} \end{bmatrix} = \begin{bmatrix} \lambda_{11}(u) & \lambda_{12}(u) & \dots & \lambda_{1r}(u) \\ \lambda_{21}(u) & \lambda_{22}(u) & \dots & \lambda_{2r}(u) \\ \vdots & \vdots & \ddots & \vdots \\ \lambda_{r1}(u) & \lambda_{r2}(u) & \dots & \lambda_{rr}(u) \\ \vdots & \vdots & \ddots & \vdots \\ \lambda_{N1}(u) & \lambda_{N2}(u) & \dots & \lambda_{Nr}(u) \end{bmatrix} \begin{bmatrix} F_{1t} \\ F_{2t} \\ \vdots \\ F_{rt} \end{bmatrix} + \begin{bmatrix} e_{1t} \\ e_{2t} \\ \vdots \\ e_{rt} \\ \vdots \\ e_{Nt} \end{bmatrix}, \quad (10)$$

where \mathbf{Y}_t is an N -dimensional vector of time series, $\mathbf{\Lambda}(u)$ is the time-varying loading matrix with $\lambda_{ij}(u) \in L^2[0, 1]$, for $i = 1, 2, \dots, N$, and $j = 1, 2, \dots, r$. \mathbf{F}_t is the common factor, and \mathbf{e}_t is the idiosyncratic process. From (9), and the Assumption E, the structure of the covariance matrix of the process \mathbf{Y}_t is written as

$$\Gamma_Y(u) = \mathbf{\Lambda}(u)\Gamma_F\mathbf{\Lambda}'(u) + \Gamma_e, \quad \forall u \in [0, 1],$$

that means, the variance of the common component is $\Gamma_X(u) = \mathbf{\Lambda}(u)\Gamma_F\mathbf{\Lambda}'(u)$.

For the construction of the time-varying loadings estimates, we first assume that the estimator of the r common factors are obtained by PCA of the N -dimensional time series \mathbf{Y}_t . Then, functions of time-varying loadings are approximated in series of orthogonal wavelets as in (8), for a fixed resolution level $J < T$,

$$\lambda_{mn}(u) = \alpha_{00}^{(mn)}\phi(u) + \sum_{j=0}^{J-1} \sum_{k \in I_j} \beta_{jk}^{(mn)}\psi_{jk}(u). \quad (11)$$

The values of j, k vary depending on the resolution level in the wavelet decomposition. We choose the maximum resolution J , such that $2^{J-1} \leq \sqrt{T} \leq 2^J$, see [Dahlhaus et al. \(1997a\)](#) for details of this selection. In practice, the coefficients $\alpha_{00}^{(mn)}, \beta_{00}^{(mn)}, \beta_{10}^{(mn)}, \dots, \beta_{J-1, 2^{J-1}}^{(mn)}$ are obtained for a particular estimation method. In this paper, we use GLS to estimate these coefficients and to reconstruct the loadings functions.

Let $\mathbf{Y}_t = (Y_{1t}, Y_{2t}, \dots, Y_{Nt})$ be N time series with $t = 1, 2, \dots, T$ which are generated by

$$\mathbf{Y}_t = \mathbf{\Lambda}(u)\tilde{\mathbf{F}}_t + \mathbf{e}_t, \quad (12)$$

where the r common factors, $\tilde{\mathbf{F}}_t$, are estimated by principal components. Each loading function $\lambda_{mn}(u)$ is written as in (11), then when plugging each $\lambda_{mn}(u)$ into (10), we have

$$\begin{aligned}
\underbrace{\begin{bmatrix} Y_{11} \\ \vdots \\ Y_{1T} \\ \vdots \\ Y_{r1} \\ \vdots \\ Y_{rT} \\ \vdots \\ Y_{N1} \\ \vdots \\ Y_{NT} \end{bmatrix}}_{\text{vec}(\mathbf{Y})} &= \underbrace{\begin{bmatrix} \Psi_{\tilde{\mathbf{F}}}^{(1)} & \Psi_{\tilde{\mathbf{F}}}^{(2)} & \dots & \Psi_{\tilde{\mathbf{F}}}^{(r)} & \dots & \mathbf{O} & \mathbf{O} & \dots & \mathbf{O} & \mathbf{O} & \mathbf{O} & \dots & \mathbf{O} \\ \mathbf{O} & \mathbf{O} & \mathbf{O} & \mathbf{O} & \dots & \mathbf{O} & \mathbf{O} & \dots & \mathbf{O} & \mathbf{O} & \mathbf{O} & \dots & \mathbf{O} \\ \vdots & \vdots & \vdots & \vdots & \ddots & \vdots & \vdots & \vdots & \vdots & \vdots & \vdots & \vdots & \vdots \\ \mathbf{O} & \mathbf{O} & \mathbf{O} & \mathbf{O} & \dots & \Psi_{\tilde{\mathbf{F}}}^{(1)} & \Psi_{\tilde{\mathbf{F}}}^{(2)} & \dots & \Psi_{\tilde{\mathbf{F}}}^{(r)} & \mathbf{O} & \mathbf{O} & \dots & \mathbf{O} \\ \vdots & \vdots & \vdots & \vdots & \vdots & \vdots & \vdots & \vdots & \vdots & \vdots & \vdots & \vdots & \vdots \\ \mathbf{O} & \mathbf{O} & \mathbf{O} & \mathbf{O} & \dots & \mathbf{O} & \mathbf{O} & \dots & \mathbf{O} & \Psi_{\tilde{\mathbf{F}}}^{(1)} & \Psi_{\tilde{\mathbf{F}}}^{(2)} & \dots & \Psi_{\tilde{\mathbf{F}}}^{(r)} \end{bmatrix}}_{\mathbf{\Theta}} \underbrace{\begin{bmatrix} \beta^{(1)} \\ \beta^{(2)} \\ \beta^{(3)} \\ \vdots \\ \beta^{(r)} \\ \vdots \\ \beta^{(N)} \end{bmatrix}}_{\boldsymbol{\beta}} + \underbrace{\begin{bmatrix} e_{11} \\ \vdots \\ e_{1T} \\ \vdots \\ e_{r1} \\ \vdots \\ e_{rT} \\ \vdots \\ e_{N1} \\ \vdots \\ e_{NT} \end{bmatrix}}_{\text{vec}(\mathbf{e})}, \\
&\quad (13)
\end{aligned}$$

where

$$\Psi_{\tilde{\mathbf{F}}}^{(i)} = \begin{bmatrix} \phi(1/T)\tilde{F}_{i1} & \psi_{00}(1/T)\tilde{F}_{i1} & \dots & \psi_{J-1,2^J-1}(1/T)\tilde{F}_{i1} \\ \phi(2/T)\tilde{F}_{i2} & \psi_{00}(2/T)\tilde{F}_{i2} & \dots & \psi_{J-1,2^J-1}(2/T)\tilde{F}_{i2} \\ \vdots & \vdots & \ddots & \vdots \\ \phi(T/T)\tilde{F}_{iT} & \psi_{00}(T/T)\tilde{F}_{iT} & \dots & \psi_{J-1,2^J-1}(T/T)\tilde{F}_{iT} \end{bmatrix},$$

are $T \times 2^J$ matrices for $i = 1, 2, \dots, r$ and \mathbf{O} is $T \times 2^J$ null matrix.

Let $\Psi_{r\tilde{\mathbf{F}}} = [\Psi_{\tilde{\mathbf{F}}}^{(1)}, \dots, \Psi_{\tilde{\mathbf{F}}}^{(r)}]$ be a $T \times r2^J$ matrix, then

$$\mathbf{\Theta} = \mathbb{I}_N \otimes \Psi_{r\tilde{\mathbf{F}}}$$

is $NT \times Nr2^J$ matrix that depends on the estimated factors, $\tilde{\mathbf{F}}_t$, the wavelets $\psi(u)$, and the resolution level J , with vector of parameters $\boldsymbol{\beta}^{(m)} = (\beta^{(m1)}, \beta^{(m2)}, \dots, \beta^{(mr)})'$ of dimension $r2^J \times 1$ for $m = 1, 2, \dots, N$, where $\beta^{(mn)} = (\alpha_{00}^{(mn)}, \beta_{00}^{(mn)}, \beta_{10}^{(mn)}, \dots, \beta_{J-1,2^J-1}^{(mn)})'$.

Each $\boldsymbol{\beta}^{(m)}$ is composed by the wavelets coefficients of the m -th row of the matrix $\mathbf{\Lambda}(u)$. Therefore, the total number of wavelets parameters to be estimated is $2^J Nr$.

Hence, the model in (13) can be represented in a linear model form as

$$\text{vec}(\mathbf{Y}) = \mathbf{\Theta}\boldsymbol{\beta} + \text{vec}(\mathbf{e}),$$

where $\text{vec}(\mathbf{Y})$ is the response vector and $\mathbf{\Theta}$ is the usual design matrix in regression analysis. Assuming that the covariance matrix of the idiosyncratic errors, Γ_e , is known, then the GLS estimator of the coefficients $\boldsymbol{\beta}$ is given by

$$\hat{\boldsymbol{\beta}} = (\mathbf{\Theta}'\Sigma_e^{-1}\mathbf{\Theta})^{-1}\mathbf{\Theta}'\Sigma_e^{-1}\text{vec}(\mathbf{Y}),$$

where Σ_e is a $NT \times NT$ matrix defined as

$$\Sigma_e = \Gamma_e \otimes \mathbb{I}_T = \begin{bmatrix} \mathbb{I}_T \gamma_{e,11} & \mathbb{I}_T \gamma_{e,12} & \cdots & \mathbb{I}_T \gamma_{e,1N} \\ \mathbb{I}_T \gamma_{e,21} & \mathbb{I}_T \gamma_{e,22} & \cdots & \mathbb{I}_T \gamma_{e,2N} \\ \vdots & \vdots & \ddots & \vdots \\ \mathbb{I}_T \gamma_{e,N1} & \mathbb{I}_T \gamma_{e,N2} & \cdots & \mathbb{I}_T \gamma_{e,NN} \end{bmatrix}.$$

These results provide linear estimators of wavelet coefficients for the time-varying loadings assuming that the covariance matrix of the idiosyncratic error is known. Some procedures, such as maximum likelihood methods, are not computationally efficient for estimating such a model since the number of parameters tends to be very large. In this light, we use GLS to simplify the implementation.

Note that we can use a different basis of wavelet functions $\phi(u)$, and $\psi_{jk}(u)$ for each $\lambda_{mn}(u)$. In the simulation section, we use a similar basis to simplify the exposition.

3.1 Estimation algorithm

The estimation algorithm is as follows:

Step 1. Use principal components to estimate \mathbf{F}_t as

$$\tilde{\mathbf{F}} = \sqrt{T}[v_1, v_2, \dots, v_r],$$

where v_i is the eigenvector corresponding to the i -th largest eigenvalue, λ_i for $i = 1, \dots, r$, of the matrix $(NT)^{-1} \mathbf{Y} \mathbf{Y}'$. Here, \mathbf{Y} and $\tilde{\mathbf{F}}$ denote $T \times N$ and $T \times r$ matrices, respectively. Next, the loading function matrix, $\Lambda(t)$, is approximated by wavelets

$$\lambda_{mn}(t) = \alpha_{00}^{(mn)} \phi(t) + \sum_{j=0}^{J-1} \sum_{k \in I_j} \beta_{jk}^{(mn)} \psi_{jk}(t),$$

with $I_j = \{k : k = 0, 1, \dots, 2^j - 1\}$, $m = 1, \dots, N$, and $n = 1, \dots, r$. Then, we write the equation (12) as

$$\text{vec}(\mathbf{Y}) = \Theta(\tilde{\mathbf{F}}, \psi, \phi) \beta + \text{vec}(\mathbf{e}),$$

where $\text{vec}(\mathbf{Y})$ and $\text{vec}(\mathbf{e})$ are $NT \times 1$ vectors, and the dimensions of $\Theta(\tilde{\mathbf{F}}, \psi, \phi)$ and β are $(NT \times 2^J Nr)$ and $(2^J Nr \times 1)$, respectively, where J indicates the resolution level chosen in the wavelet expansions.

Step 2. Estimate by GLS the wavelet coefficients as

$$\hat{\beta} = (\Theta' \Sigma_e^{-1} \Theta)^{-1} \Theta' \Sigma_e^{-1} \mathbf{Z},$$

where $\Theta(\tilde{\mathbf{F}}, \psi, \phi) \equiv \Theta$, $\mathbf{Z} = \text{vec}(\mathbf{Y})$, and $\Sigma_e = \mathbb{I}_{NT}$ is used as initial value.

Step 3. Using the estimated coefficient in the Step 2, the loadings are obtained as

$$\hat{\mathbf{\Lambda}}(t)^{(0)} = \{\hat{\lambda}_{mn}^{(0)}(t)\}_{m=1,\dots,N}^{n=1,\dots,r},$$

where

$$\hat{\lambda}_{mn}^{(0)}(t) = \hat{\alpha}_{00}^{(mn)}\phi(t) + \sum_{j=0}^{J-1} \sum_{k \in I_j} \hat{\beta}_{jk}^{(mn)}\psi_{jk}(t).$$

Step 4. With $\hat{\mathbf{\Lambda}}(t)^{(0)}$, obtain residuals, $\mathbf{Y}_t - \hat{\mathbf{\Lambda}}(t)^{(0)}\tilde{\mathbf{F}}_t = \hat{\mathbf{e}}_t^{(0)}$. Then, compute

$$\hat{\Gamma}_e^{(0)} = \sum_{t=1}^T \hat{\mathbf{e}}_t^{(0)}\hat{\mathbf{e}}_t^{(0)'} / T.$$

Step 5. Back to step 2 with $\Sigma_e = \hat{\Gamma}_e^{(0)}$. Iterate n -times the procedure to obtain the sequences $\{\hat{\mathbf{\Lambda}}(t)^{(i)}, \hat{\Gamma}_e^{(i)}\}_{i=1,\dots,n}$. Stop the iteration when

$$\|\hat{\mathbf{\Lambda}}(t)^{(i-1)} - \hat{\mathbf{\Lambda}}(t)^{(i)}\| < \delta,$$

for any small $\delta > 0$, where $\|\cdot\|$ denotes the Frobenius norm for $t = 1, \dots, T$.

It is possible to improve the efficiency of the common factors by giving the new value of the loading matrix, regressing the series on loadings to obtain a new estimate of the factors, and then iterate the algorithm. However, this procedure is computationally very intensive for large data sets. As shown in the following two sections, it is unnecessary to implement an expensive iterative procedure to get successful results. Our algorithm is comparable with the methodology proposed by [Mikkelsen et al. \(2018\)](#), which also does not iterate the algorithm.

4 Monte Carlo simulation

We examine the finite-sample properties of the estimation procedure proposed above using a Monte Carlo study. The model in (1) is generated as

$$\begin{aligned} Y_{it} &= \boldsymbol{\lambda}'_i(t)\mathbf{F}_t + e_{it}, \quad i = 1, \dots, N \quad \text{and} \quad t = 1, \dots, T, \\ F_{kt}(1 - \theta_k L) &= \eta_{kt}, \quad k = 1, \dots, r. \quad \boldsymbol{\eta}_t \sim \mathcal{N}_r(0, \text{diag}\{\beta_1^2, \dots, \beta_r^2\}), \\ \mathbf{e}_t &\sim \mathcal{N}_N(0, \Gamma_e), \end{aligned}$$

where L is the lag operator, $|\beta_i| < 1$, for $i = 1, \dots, r$, and the matrix Γ_e is generated by two structures; i) $\Gamma_e = \{\gamma^{|i-j|}\}_{i,j=1,\dots,N}$, a Toeplitz matrix, and ii) a diagonal matrix. Furthermore, at time t , Y_{it} denotes the i -th time series, $\boldsymbol{\lambda}'_i(t) = (\lambda_{i1}(t), \dots, \lambda_{ir}(t))$ is vector of loadings, which are alternately generated by some smooth functions. We discuss a couple of functions used below. $\mathbf{F}_t = (F_{1t}, \dots, F_{rt})'$ is the vector of factors, and $\boldsymbol{\eta}_t = (\eta_{1t}, \dots, \eta_{rt})'$ factor errors and

$\mathbf{e}_t = (e_{1t}, \dots, e_{Nt})'$ are vectors of idiosyncratic terms which are independent to each other.

A referee kind let us know that Gaussian distributions for both error terms in our Monte Carlo experiment can be relaxed by incorporating other types of distributions. The referee points out that assuming homogeneous distributions on $[F_{min}, F_{max}]$ can help the model be more accurate in some empirical applications. As commented by the referee, a possible estimation method can be the wavelet polynomial chaos method.

Another possibility to explore our model under a non-Gaussian distribution could be under the state-space modeling. As pointed in [Durbin and Koopman \(2012\)](#), it is common to assume normality distribution in the innovation in state-space models because the model is estimated by maximizing a Gaussian log-likelihood, which is evaluated by the Kalman filter. In principle, quasi-maximum likelihood methods can be used when actual distributions of the error terms are non-Gaussian. The possibility of non-Gaussian distributions is beyond the scope of the present paper and is not further explored. [Poncela et al. \(2021\)](#) provide an excellent survey on factor extraction using Kalman filter.

In our Monte Carlo study, the model is generated with $N \in \{20, 30, 100\}$ cross-sectional units and $T \in \{512, 1024, 2048\}$ sample sizes. We consider for simplicity only two common factors ($r = 2$). Furthermore, three values for $\theta_k \in \{0, 0.5, 1\}$ for $k = 1, 2$, are considered. Two values for Γ_e ; a Toeplitz matrix $\Gamma_e = Toep$ with $\gamma = 0, 7$ for correlated noise and $\Gamma_e = Diag$ for uncorrelated, where a uniform distribution $U(0.5, 1.5)$ generates the entries of the diagonal matrix. Note that simulated data are standardized before extracting the principal components. Common factors are estimated by principal components in cases with $\theta_k < 1$, and by the procedure of [Peña and Poncela \(2006\)](#) in the case with $\theta_k = 1$. All simulations are based on 1000 replications of the model.

We rotate the obtained factors to compare proposed estimations with the actual factors. The optimal rotation A^* is obtained by maximizing $tr[corr(\mathbf{F}, \tilde{\mathbf{F}}A)]$. The solution is given by $A^* = VU$ where V and U are orthogonal matrices of the decomposition $corr(F, \tilde{F}) = USV'$. When the number of k principal components is not equal to the number of factors r , we rotate the first $l = \min\{k, r\}$ principal components, see [Eickmeier et al. \(2015\)](#). Both estimated and simulated factors are re-scaled to keep the same standard deviation, then

$$\tilde{\mathbf{F}}_k^* = \frac{\sigma(F_k)}{\sigma(\tilde{F}_k)} \tilde{\mathbf{F}}_k, \quad k = 1, \dots, r, \quad (14)$$

where $\tilde{\mathbf{F}}_k$ is the k -th column of the matrix of the rotated principal components $\tilde{\mathbf{F}}A^*$.

As explained before, these rotated factors are now treated as observed variables in the regression model

$$vec(\mathbf{Y}) = \Theta(\tilde{\mathbf{F}}^*, \psi, \phi)\beta + vec(\mathbf{e}),$$

to estimate the wavelet coefficients, β , where $\tilde{\mathbf{F}}^* = (\tilde{\mathbf{F}}_1^*, \dots, \tilde{\mathbf{F}}_r^*)$.

To investigate the performance of the estimation procedure, estimated and simulated factors are compared as follows:

- i) The precision of the estimation factors is measured by the $R_{\tilde{F},F}^2$ statistics as in [Bates et al. \(2013\)](#), given by

$$R_{\tilde{F},F}^2 = \frac{\text{tr}[\mathbf{F}'\tilde{\mathbf{F}}(\tilde{\mathbf{F}}'\tilde{\mathbf{F}})^{-1}\tilde{\mathbf{F}}'\mathbf{F}]}{\text{tr}[\mathbf{F}'\mathbf{F}]}, \quad (15)$$

where $\tilde{\mathbf{F}}$ is the $T \times r$ matrix of estimated factors as in (14) and \mathbf{F} is the $T \times r$ matrix of the actual factors, that is the simulated ones. This statistics is a multivariate R^2 in a regression of the actual factors on the principal components. When the canonical correlation of the actual and estimated factors tends to one, then $R_{\tilde{F},F}^2 \rightarrow 1$ as well.

- ii) We measure the precision of loadings estimates by mean square errors (MSE) between estimated and actual loadings, as in [Motta et al. \(2011\)](#). The MSE is computed as follows

$$MSE(v) = (NT)^{-1} \sum_{t=1}^T \|\hat{\mathbf{\Lambda}}^{(v)}(t) - \mathbf{\Lambda}(t)\|,$$

for $v = 1, \dots, 1000$. The estimator of the factor loadings matrix, $\mathbf{\Lambda}(t)$, is chosen by a path such that

$$\hat{\mathbf{\Lambda}}(t) = \{\hat{\mathbf{\Lambda}}^{(m)}(t) : MSE_m = \text{median}\{MSE(1), \dots, MSE(1000)\}\}. \quad (16)$$

Table 1 shows the results of the estimations of (15) and (16). As can be seen, the methodology proposed in this paper performs very well in relatively small samples regardless of size distortion between N and T . As seen in Table 1, $R_{\tilde{F},F}^2$ is relatively high, indicating the satisfactory performance of the estimator. However, precision is a bit reduced when increasing the value of θ . These findings are maintained for both types of wavelets used and even when we allow for cross-correlation between idiosyncratic errors. Furthermore, inspecting the MSE in Table 1, we find that the MSEs decrease as T increases in all cases, even if the common factors are serially correlated or if idiosyncratic errors are cross-correlated. Furthermore, another finding indicates that, in general, factor loadings using the wavelet D8 perform better than the wavelet Haar. We think that such results are reasonable due to the smoothness of the wavelet D8 in contrast with the other one. The wavelet Haar should be implemented when factor loadings' dynamic have breaks or perhaps some aggressive jumps. We do not go any further in this line. Wavelet Haar's features are part of another research and are out of the present scope.

Furthermore, in Figures 1 and 2, we display the methodology's performance to estimate the factor loadings. We choose a couple of different smooth functions

Table 1: $T \in \{512, 1024, 2048\}$, $N \in \{20, 30, 100\}$, and $r = 2$. The measure of the consistency of the estimated unobservable factors and the estimated factor loadings are presented in the report.

		Wavelet functions											
		Haar						D8					
N	T	Γ_e	$R^2_{\hat{F},F}$	MSE_m	$R^2_{\hat{F},F}$	MSE_m	$R^2_{\hat{F},F}$	MSE_m	$R^2_{\hat{F},F}$	MSE_m	$R^2_{\hat{F},F}$	MSE_m	$R^2_{\hat{F},F}$
20	512	Diag	0.9341	0.0103	0.8042	0.1970	0.7450	0.1562	0.9047	0.0111	0.8655	0.0023	0.7314
	1024		0.9421	0.0076	0.8135	0.0900	0.7501	0.1202	0.9347	0.0082	0.8764	0.0011	0.7439
	2048		0.9432	0.0018	0.8237	0.0052	0.7840	0.0711	0.9470	0.0005	0.8855	0.0009	0.8046
30	512	Diag	0.9236	0.0098	0.8056	0.0128	0.7091	0.1091	0.9460	0.0071	0.8521	0.0127	0.7931
	1024		0.9547	0.0051	0.8125	0.0090	0.7112	0.0859	0.9487	0.0047	0.8671	0.0079	0.7963
	2048		0.9723	0.0015	0.8268	0.0027	0.7324	0.0738	0.9498	0.0020	0.8691	0.0059	0.8213
100	512	Diag	0.9062	0.0088	0.8019	0.0147	0.7014	0.1198	0.9643	0.0062	0.8674	0.0102	0.8984
	1024		0.9100	0.0042	0.8418	0.0081	0.7020	0.0781	0.9701	0.0037	0.9044	0.0081	0.9105
	2048		0.9241	0.0017	0.8857	0.0035	0.7153	0.0719	0.9812	0.0025	0.9202	0.0054	0.9300
20	512	Toep	0.8631	0.0672	0.6932	0.0891	0.6711	0.2201	0.8911	0.0128	0.6871	0.0593	0.6242
	1024		0.8634	0.0501	0.6953	0.0702	0.7012	0.1901	0.8926	0.0100	0.7001	0.0337	0.6832
	2048		0.8911	0.0137	0.7723	0.0433	0.7321	0.1642	0.8971	0.0091	0.7307	0.0108	0.6941
30	512	Toep	0.8531	0.0472	0.7984	0.0621	0.6812	0.0912	0.9021	0.0117	0.6815	0.0311	0.7483
	1024		0.8671	0.0231	0.7730	0.0539	0.7122	0.0734	0.9126	0.0090	0.7270	0.0276	0.7126
	2048		0.8711	0.0092	0.8200	0.0311	0.7212	0.0819	0.9232	0.0068	0.7305	0.0109	0.7531
100	512	Toep	0.8503	0.0398	0.8081	0.0510	0.7294	0.0831	0.9368	0.0101	0.7902	0.0263	0.7566
	1024		0.8602	0.0288	0.7942	0.0495	0.7413	0.0698	0.9404	0.0087	0.8012	0.0201	0.7774
	2048		0.8893	0.0104	0.8491	0.0209	0.7629	0.0503	0.9499	0.0070	0.8125	0.0117	0.7849

Notes: The DGP is $Y_{it} = \mathbf{\lambda}'_i(t)\mathbf{F}_t + e_{it}$, where $i \in \{20, 30, 100\}$ and $T \in \{512, 1024, 2048\}$, $F_{kt}(1 - \theta_k B) = \eta_{kt}$, with $k \in \{1, 2\}$. Idiosyncratic terms are independently generated as $\eta_t \sim \mathcal{N}_1(0, \text{diag}\{\beta_1^2, \beta_2^2\})$ with $|\beta_i| < 1$, for $i = 1, 2$ and $\theta_k \in \{0, 0.5, 1\}$ defining the degree of serial correlation among factors, and $e_t \sim \mathcal{N}_N(0, \Gamma_e)$ with Γ_e defined as diagonal and Toeplitz matrices. Common factors are estimated by principal components in cases with $\theta_k < 1$, and by the procedure of [Peña and Poncela \(2006\)](#) in the case with $\theta_k = 1$. $R^2_{\hat{F},F}$ is the R^2 of a regression of actual on estimates factors. MSE_m is the median of the MSE between the actual and estimated factor loadings. Haar and D8 wavelet functions are used in the study. All experiments are based on 1000 replications.

for each value of θ and in both types of wavelets for comparison purposes. We consider the following functions: i) $\lambda_{1,12}(t) = 0.4 \cos -3\pi t$, and ii) $\lambda_{2,8}(t) = 0.6(0.7\sqrt{t} - 0.5 \sin 1.2\pi t)$, where $\lambda_{1,12}$ indicates the loading of the first factor of the cross-sectional unit $i = 12$, and $\lambda_{2,8}$, the loadings of the second factor of unit $i = 8$. Figures display the actual and estimated time-varying loadings and their bootstrap confidence interval at 95% with $B = 100$ replications, following [de A. Moura et al. \(2012\)](#). In such figures, we can see that the methodology works well independently of the value taken in θ_k .

Finally, as a complement of this simulation study, we compare our methodology with the approach of [Mikkelsen et al. \(2018\)](#). Their estimation methodology is similar to ours in the first stage. The difference is in the second stage because instead of using wavelet functions, as in this paper, they employ Kalman filter procedures to estimate the likelihood function. It is worth mentioning that the main difference between both setups lies in the performance of loading factors. While we assume smooth variations in this paper, their approach consists of stationary VAR processes.

We use the same DGP as before, but we focus only on the following simplest case.

$$\begin{aligned} Y_{it} &= \boldsymbol{\lambda}'_i(t) \mathbf{F}_t + e_{it}, \quad i = 1, \dots, 20 \quad \text{and} \quad t = 1, \dots, 512, \\ F_t &= \eta_t, \quad \text{where } \eta_t \sim \mathcal{N}(0, 1), \\ \mathbf{e}_t &\sim \mathcal{N}_N(0, \Gamma_e), \end{aligned}$$

where the matrix Γ_e is a diagonal matrix, and idiosyncratic terms are independent of each other. As before, the vector of loadings is generated alternately by some smooth functions. We split them into two groups; i) smooth sine/cosine functions and ii) smooth trending functions (linear, square root, exponential, and logs trends).

Our analysis finds that the methodology proposed by [Mikkelsen et al. \(2018\)](#) does not adjust either smooth sinusoidal functions or smooth trending functions in most cases. The worst performance appears when loadings are trending functions, while it is possible to rescue from time to time some proper estimations when loadings behave as sine/cosine functions. Given our results, we argue that the model proposed in this paper seems to be more suitable when loadings have deterministic trends; in contrast, the methodology proposed by [Mikkelsen et al. \(2018\)](#) fails to capture this type of behavior in loadings by treating them as a stationary VAR.

We repeated the entire simulation study as in Table 1 using the methodology of [Mikkelsen et al. \(2018\)](#); however, given the inferior performance of loading estimates, we prefer not to augment Table 1 for brevity. Instead, we support this part of the simulation study with Figure 1 that compares both approaches with four examples of smooth functions, two cases when loadings have trends, and two with sinusoidal functions.

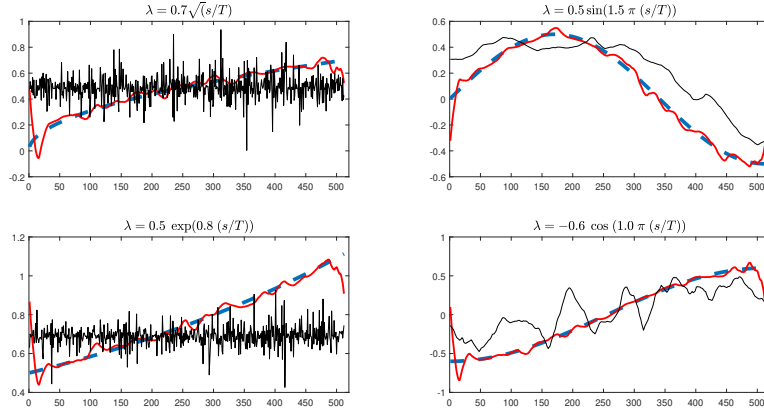


Figure 1: Comparison between the methodology proposed in this paper (solid red line) and that by Mikkelsen et al. (2018) (solid black line) to estimate time-varying loadings (dashed blue line) defined by the smooth function written above of each figure.

5 Application

This section applies our methodology to study comovements in loads and prices of the Nord Pool power market.

Nord Pool runs the leading power market in Europe and operates in the day-ahead and intraday markets. Elspot is the day-ahead auction market, where participants act in a double auction and submit their supply and demand orders (spot prices and loads) for each hour of the next day. The market is in equilibrium when demand and supply curves intersect at the system price and system load for each hour. The hourly system prices and loads series are announced as 24-dimensional vectors, which are determined simultaneously.

Electricity markets have particular features that do not exist in any other commodity market. Remarkably, the non-storability of electricity provokes that the time series of prices shows excessive volatility, possible negative prices, and many spikes over time. Other relevant features of electricity prices and loads are the intra-day, week, and year seasonal components, see Weron (2007).

Univariate time series methods have mostly studied hourly electricity prices and loads, see Weron (2014) for a rich review. Some authors have explored these series by multivariate techniques as high dimensional factor models until the last years. Using data from the Iberian Electricity Market (MIBEL), seasonal factors have been extracted in the works of Alonso et al. (2011) and Garcia-Martos et al. (2012), whereas Alonso et al. (2016) propose to employ model averaging factor models to improve forecasting performance. Pennsylvania - New Jersey - Maryland (PJM) interconnection market is studied by Maciejowska and Weron (2015) who estimate factor models for forecasting evaluation using hourly and

zonal prices. Furthermore, the Nord Pool power market is studied in the works of [Ergemen et al. \(2016\)](#), who study the long-term relationship between system prices and loads, and [Rodríguez-Caballero and Ergemen \(2017\)](#), who use regional prices in a multi-level setting.

All these studies assume that factor loadings do not vary over time. In this sense, we are the first to study the power market with a factor model with time-varying loadings to the best of our knowledge. Such a setup may help to attract some dynamics not necessarily captured in common factors. We argue that factor loadings should evolve smoothly, perhaps reacting to the auction market's smooth changes along the day and along year due to the series' inherent seasonality.

We consider a balanced panel data set consisting of $N = 24$ hourly prices and loads for each day from 13th March 2016 to 31st December 2018, yielding a total of $T = 1024$ daily observations in each hour. We download series from the Nord Pool ftp server, and prices are in Euros per Mwh of a load. Figures 2 and 3 display six time series in logs from which we can observe some characteristics in both time series. First, electricity system prices and loads vary differently along months with a common pattern in their evolutions. Second, the price series show many spikes which are related to the way how the market operates. Third, seasonal variations are much more marked in loads than in price series. Fourth, electricity prices and loads seem to have nonstationary behaviors, then, we set our estimation on the nonstationary approach discussed in section 2.2.

We use the procedure proposed by [Alessi et al. \(2010\)](#) with first-differenced variables to estimate the number of factors. This methodology introduces a multiplicative tuning constant in the penalty function to improve the criteria of [Bai and Ng \(2002\)](#). In line with the literature, we find two common factors in prices, and the same number in loads. These factors explain 95% of the variation in the panel of prices, and 97% of loads. These percentages are slightly higher than those found in [Ergemen et al. \(2016\)](#), but our period is shorter and does not cover periods of infrastructure delineation in the Nord Pool power market. Therefore, we estimate the model in (12) with two common factors for the panel of loads and the panel of prices.

Figures 4 and 5 display estimates of common factors of hourly system loads and prices, respectively. As seen in Figure 4, the first factor of hourly loads captures the strong seasonal component showing possible weekly and monthly periodicities. The second factor seems to capture mainly a more erratic weekly variability, mostly during working hours, as seen in Figure 2. On the other hand, Figure 5 shows that estimated common factors of hourly system prices exhibit some stylized facts of the underlying series. Volatility clustering and nonstationary behavior are captured by the first factor, while excessive price spikes in 2018 by March, July, and August are extracted mostly by the second factor. [Ergemen et al. \(2016\)](#) also document all these characteristics of common factors.

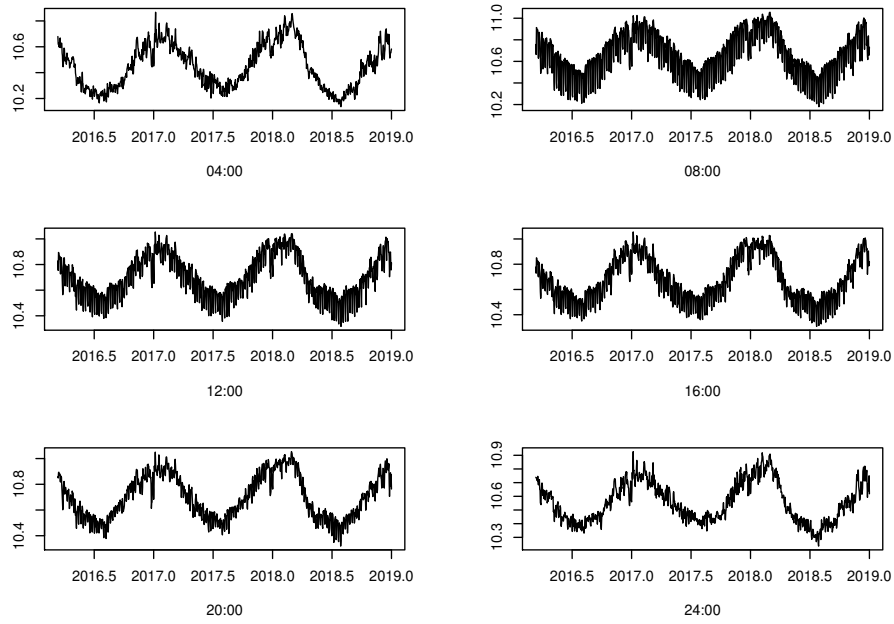


Figure 2: Hourly system loads in logs for six different hours showing working and non-working hours performances, 12 March 2016 to 31 December 2018.

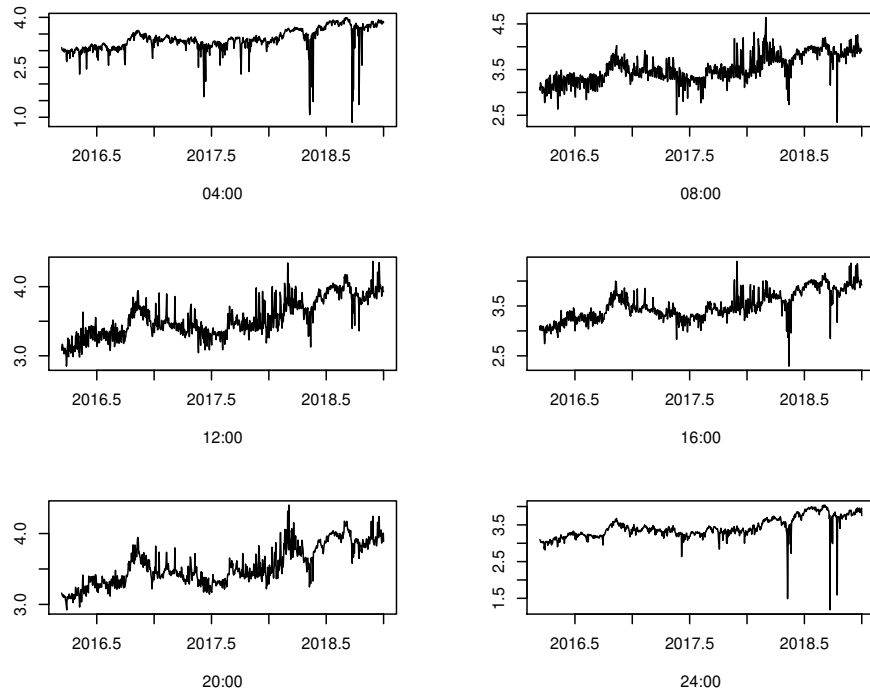


Figure 3: Hourly system prices in logs for six different hours showing working and non-working hours performances, 12 March 2016 to 31 December 2018.

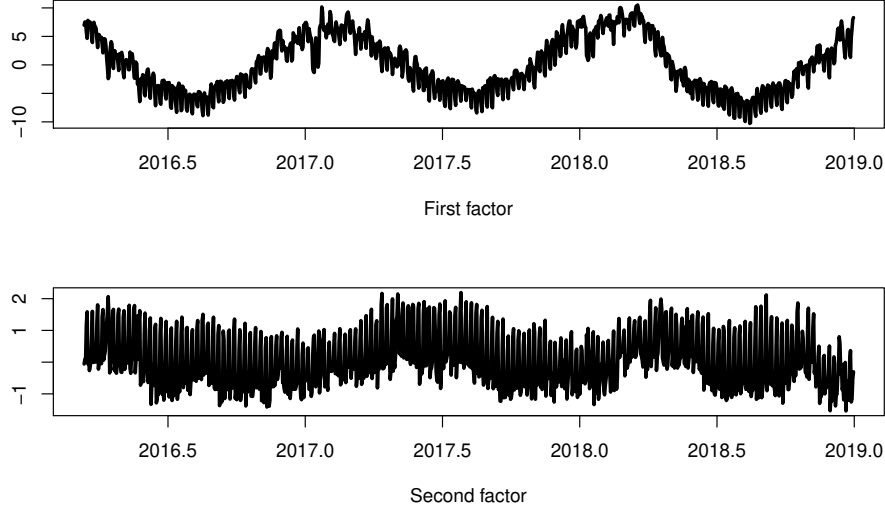


Figure 4: Common factors of hourly system loads.

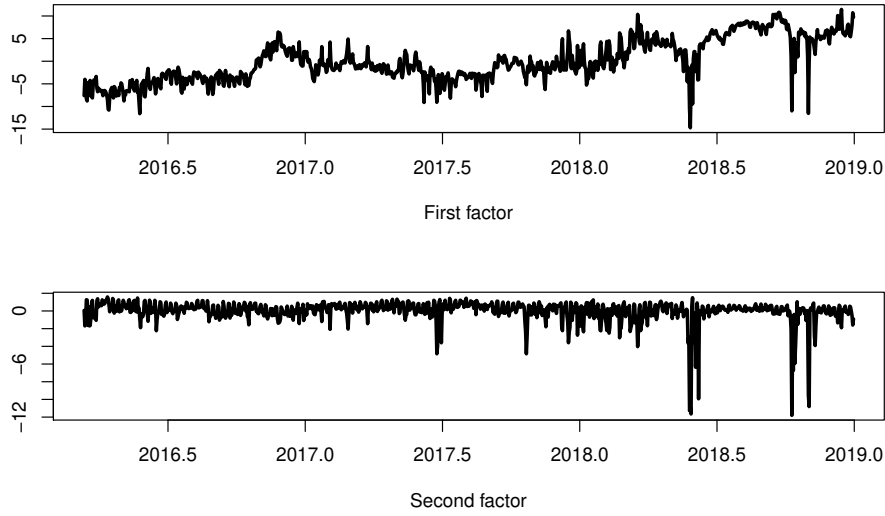


Figure 5: Common factors of hourly system prices.

Figures 6 and 7 show time-varying loadings of the first and second common factors of hourly system loads, respectively. Figures 8 and 9 show the time-varying loadings estimates of hourly system prices. We only display the results for six hours for exposition purposes: 04:00, 08:00, 12:00, 16:00, 20:00, and 24:00 hrs. These hours help to observe different performances of loadings across working and non-working hours. For comparison purposes, we estimate the model proposed by

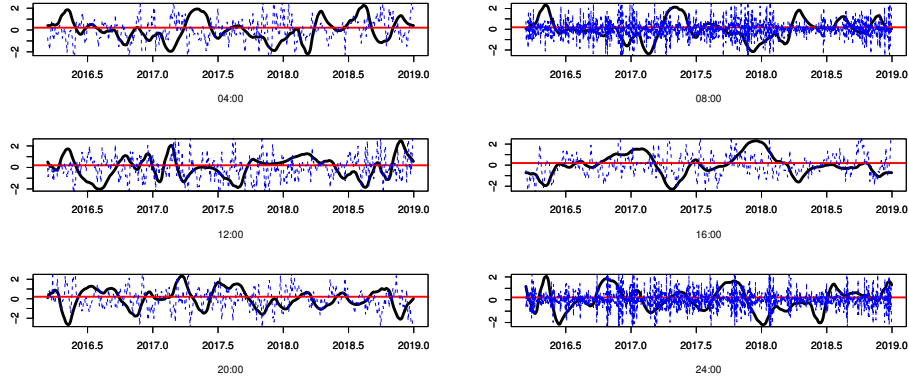


Figure 7: Time-varying loadings of the second factor of hourly system loads. Black solid lines represent loadings estimated by the method proposed in this paper, while blue dot lines represent loadings estimated by [Mikkelsen et al. \(2018\)](#).

[Mikkelsen et al. \(2018\)](#) using the generalized covariance matrix introduced in (5), in the first stage, to allow for nonstationary variables. We standardized loadings estimates to compare both approaches.

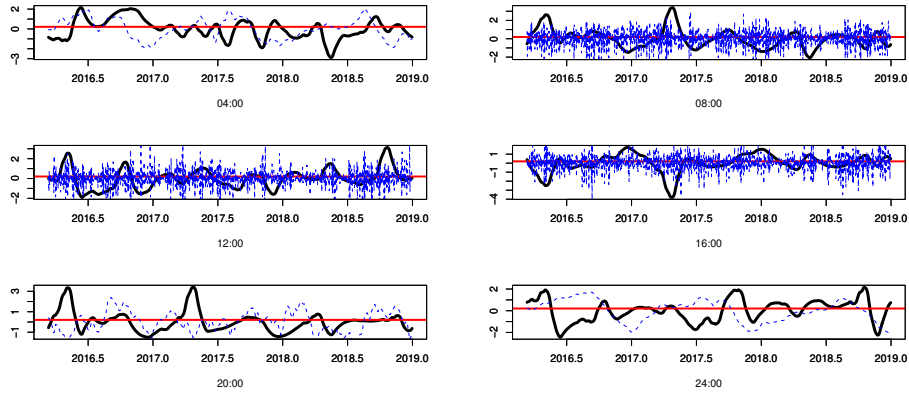


Figure 6: Time-varying loadings of the first factor of hourly system loads. Black solid lines represents loadings estimated by the method proposed in this paper, while blue dot lines represents loadings estimated by [Mikkelsen et al. \(2018\)](#).

Further inspection on Figure 6 indicates that factor loadings corresponding to the first common factor of system loads show smooth variations along time when estimating them by the model proposed in this paper (solid black lines in figures). These time-varying loadings capture a kind of readjustment of system loads when the demand reaches a maximum level (in winter) and a minimum level (in summer), which aligns with the market's nature. Moreover, time-varying loadings in the remaining months oscillate smoothly around the mean. In contrast, factor loadings

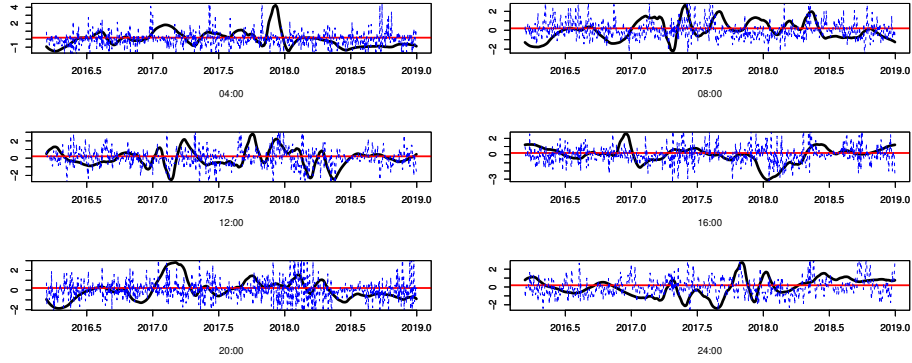


Figure 8: Time-varying loadings of the first factor of hourly system prices. Black solid lines represent loadings estimated by the method proposed in this paper, while blue dot lines represent loadings estimated by [Mikkelsen et al. \(2018\)](#).

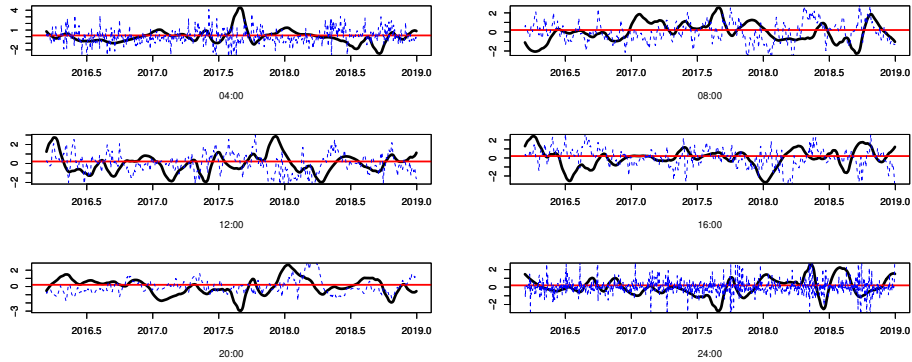


Figure 9: Time-varying loadings of the second factor of hourly system prices. Black solid lines represent loadings estimated by the method proposed in this paper, while blue dot lines represent loadings estimated by [Mikkelsen et al. \(2018\)](#).

by [Mikkelsen et al. \(2018\)](#) (blue dot lines) behave smoothly during non-working hours (see, 04:00, 20:00, and 24:00 hrs.), but the performance is very erratic during working hours (see, 08:00, 12:00, and 16:00 hrs.). Our intuition says that such erratic behavior comes from the volatile behavior of the hourly loads in the same working hours (see again Figure 2). Therefore, the main difference between both approaches appears in hours when series behave more volatile. However, it seems intuitive to think that factor loadings should behave smoothly throughout the year without considering the time of day because of changes in the electricity demand.

In turn, factor loadings corresponding to the second common factor of system loads also have a regular periodic behavior along time, see solid black lines Figure 7. It is interesting to see that loadings behave smoothly independently if the second common factor is much more volatile than the first one (see Figure 4). In contrast, the second approach (blue dot lines in the figure) reacts aggressively along time and could be related to the performance of the second common factor.

Concerning loadings estimates of hourly system prices using the methodology proposed in this paper (solid black lines in Figure 8), at first glance, unlike system loads, we do not find that factor loadings have precise periodic movements along time. In general, they also behave smoothly as before. It is worth mentioning that some moments where loadings seem to be time-invariant, see, for instance, the last year in Figure 6. Note that this behavior is not captured by loadings estimates using the approach of [Mikkelsen et al. \(2018\)](#) (see blue dot lines in the same figures), which provides loadings with a very volatile performance.

This empirical study leaves many open possibilities for future research. First, testing if loadings are time-varying or constant over time. This test would improve the specification of factor models and help to understand the market behavior. Second, short-term forecasting of prices and loads is essential for energy markets. Therefore, another research may investigate if loads/prices forecasts obtained by time-varying factor models are more accurate than those provided by standard setups. Third, as discussed in the Monte Carlo study, the factor loadings using the wavelet D8 perform better than Haar in situations where time-series evolve smoothly, as in the case of system loads. In this sense, a deeper study on electricity prices could help us understand if the wavelet Haar represents a better choice for modeling the performance of factor loadings since electricity prices are more volatile than loads.

To conclude, our setup and methodology can be used in panel data models where unobservable common factors drive the cross-sectional dependence. Recently, [Rodríguez-Caballero et al. \(2020\)](#) explored this possibility to analyze the dynamic behind air pollution and mobility to disentangle the contagion in the COVID pandemic.

6 Concluding remarks

Factor models' standard approaches assume that factor loadings are invariant along time. Here, we relaxed such an assumption allowing for time-varying loadings that behave as smooth and continuous-time functions. The paper is novel because time-varying can capture a more realistic behavior compared to some proposals in the literature that assume that stable stochastic processes drive loadings. Our estimation methodology is a two-step procedure based on GLS with wavelet functions. We explored stationary and nonstationary setups to the extent of the model's applicability. We recommend using Wavelet D8 estimates in empirical applications with smoothed loadings based on our finite sample analysis. In this sense, Wavelet D8 provides better estimations than Wavelet Haar when factor loadings do not have sudden changes.

Finally, in our empirical study, we focus on the complex dynamics of Nord Pool electricity loads and prices in a large panel of hourly observations. Our findings indicate that factor loadings vary smoothly over time in prices and loads. Notably, in loads, the time-varying loadings have a periodic behavior, which obeys the market's seasonality. The analysis provides relevant insights into the dynamics of the market. Future research will point to how the model proposed can be used from a forecasting perspective.

References

- Alessi, L., Barigozzi, M., and Capasso, M. (2010). Improved penalization for determining the number of factors in approximate factor models. *Statistics & Probability Letters*, 80(23):1806–1813.
- Alonso, A., Bastos, G., and García-Martos, C. (2016). Electricity price forecasting by averaging dynamic factor models. *Energies*, 9(8):600.
- Alonso, A. M., García-Martos, C., Rodríguez, J., and Jesús Sánchez, M. (2011). Seasonal dynamic factor analysis and bootstrap inference: application to electricity market forecasting. *Technometrics*, 53(2):137–151.
- Bai, J. (2003). Inferential theory for factor models of large dimensions. *Econometrica*, pages 135–171.
- Bai, J. and Han, X. (2016). Structural changes in high dimensional factor models. *Frontiers of Economics in China; Beijing*, 11(1):9–39.
- Bai, J. and Li, K. (2016). Maximum likelihood estimation and inference for approximate factor models of high dimension. *Review of Economics and Statistics*, 98(2):298–309.
- Bai, J. and Ng, S. (2002). Determining the number of factors in approximate factor models. *Econometrica*, 70(1):191–221.
- Bai, J. and Ng, S. (2004). A panic attack on unit roots and cointegration. *Econometrica*, 72(4):1127–1177.
- Bai, J., Ng, S., et al. (2008). Large dimensional factor analysis. *Foundations and Trends® in Econometrics*, 3:89–163.
- Barigozzi, M., Lippi, M., and Luciani, M. (2016). Non-stationary dynamic factor models for large datasets. *arXiv preprint arXiv:1602.02398*.
- Bates, B. J., Plagborg-Møller, M., Stock, J. H., and Watson, M. W. (2013). Consistent factor estimation in dynamic factor models with structural instability. *Journal of Econometrics*, 177(2):289–304.
- Chan, N. H., Lu, Y., and Yau, C. Y. (2017). Factor modelling for high-dimensional time series: Inference and model selection. *Journal of Time Series Analysis*, 38(2):285–307.
- Chiann, C. and Morettin, P. A. (2005). Time-domain estimation of time-varying linear systems. *Journal of Nonparametric Statistics*, 17(3):365–383.
- Cohen, A. and Ryan, R. D. (1995). *Wavelets and multiscale signal processing*. Springer.

- Dahlhaus, R., Eichler, M., and Sandkühler, J. (1997a). Identification of synaptic connections in neural ensembles by graphical models. *Journal of neuroscience methods*, 77(1):93–107.
- Dahlhaus, R. et al. (1997b). Fitting time series models to nonstationary processes. *The annals of Statistics*, 25(1):1–37.
- de A. Moura, M. S., Morettin, P. A., Toloi, C. M. C., and Chiann, C. (2012). Transfer function models with time-varying coefficients. *Journal of Probability and Statistics*, 2012:31.
- Durbin, J. and Koopman, S. J. (2012). *Time series analysis by state space methods*. Oxford university press.
- Eichler, M., Motta, G., and Von Sachs, R. (2011). Fitting dynamic factor models to non-stationary time series. *Journal of Econometrics*, 163(1):51–70.
- Eickmeier, S., Lemke, W., and Marcellino, M. (2015). Classical time varying factor-augmented vector autoregressive models estimation, forecasting and structural analysis. *Journal of the Royal Statistical Society: Series A (Statistics in Society)*, 178(3):493–533.
- Ergemen, Y. E., Haldrup, N., and Rodríguez-Caballero, C. V. (2016). Common long-range dependence in a panel of hourly nord pool electricity prices and loads. *Energy Economics*, 60:79–96.
- Forni, M., Hallin, M., Lippi, M., and Reichlin, L. (2000). The generalized dynamic-factor model: Identification and estimation. *The Review of Economics and Statistics*, 82(4):540–554.
- Forni, M., Hallin, M., Lippi, M., and Reichlin, L. (2004). The generalized dynamic factor model consistency and rates. *Journal of Econometrics*, 119(2):231–255.
- Forni, M., Hallin, M., Lippi, M., and Reichlin, L. (2005). The generalized dynamic factor model: one-sided estimation and forecasting. *Journal of the American Statistical Association*, 100(471):830–840.
- Gao, Z. and Tsay, R. S. (2019). A structural-factor approach to modeling high-dimensional time series and space-time data. *Journal of Time Series Analysis*, 40(3):343–362.
- Garcia-Martos, C., Rodriguez, J., and Sanchez, M. (2012). Forecasting electricity prices by extracting dynamic common factors: application to the iberian market. *IET Generation, Transmission & Distribution*, 6(1):11–20.
- Lam, C., Yao, Q., et al. (2012). Factor modeling for high-dimensional time series: inference for the number of factors. *The Annals of Statistics*, 40(2):694–726.

- Maciejowska, K. and Weron, R. (2015). Forecasting of daily electricity prices with factor models: utilizing intra-day and inter-zone relationships. *Computational Statistics*, 30(3):805–819.
- Mikkelsen, J. G., Hillebrand, E., and Urga, G. (2018). Consistent estimation of time-varying loadings in high-dimensional factor models. *Journal of Econometrics*.
- Motta, G., Hafner, C. M., and von Sachs, R. (2011). Locally stationary factor models: Identification and nonparametric estimation. *Econometric Theory*, 27(6):1279–1319.
- Peña, D. and Box, G. E. (1987). Identifying a simplifying structure in time series. *Journal of the American statistical Association*, 82(399):836–843.
- Peña, D. and Poncela, P. (2006). Nonstationary dynamic factor analysis. *Journal of Statistical Planning and Inference*, 136(4):1237–1257.
- Poncela, P., Ruiz, E., and Miranda, K. (2021). Factor extraction using kalman filter and smoothing: This is not just another survey. *International Journal of Forecasting*.
- Porto, R., Morettin, P., and Aubin, E. C. Q. (2008). Wavelet regression with correlated errors on a piecewise holder class. *Statistics & Probability Letters*, 78(16):2739–2743.
- Rodríguez-Caballero, C. V. and Ergemen, Y. E. (2017). Estimation of a dynamic multilevel factor model with possible long-range dependence. Technical report, Universidad Carlos III de Madrid. Departamento de Estadística.
- Rodríguez-Caballero, C. V., Vera-Valdés, J. E., et al. (2020). Air pollution and mobility in the mexico city metropolitan area, what drives the covid-19 death toll? Technical report, Department of Economics and Business Economics, Aarhus University.
- Stock, J. H. and Watson, M. W. (2002). Forecasting using principal components from a large number of predictors. *Journal of the American Statistical Association*, 97(460):1167–1179.
- Su, L. and Wang, X. (2017). On time-varying factor models: Estimation and testing. *Journal of Econometrics*, 198(1):84–101.
- Vidakovic, B. (2009). *Statistical modeling by wavelets*, volume 503. John Wiley & Sons.
- Weron, R. (2007). *Modeling and forecasting electricity loads and prices: A statistical approach*, volume 403. John Wiley & Sons.

Weron, R. (2014). Electricity price forecasting: A review of the state-of-the-art with a look into the future. *International Journal of Forecasting*, 30(4):1030 – 1081.

Appendix

A Technical appendix

A.1 Proof of Theorem 1

Proof. Let $\mathbf{Y} = (Y_1, \dots, Y_T)'$ be a $T \times N$ matrix, and let V_{NT} be a $r \times r$ diagonal matrix composed by the r largest eigenvalues of the matrix $(NT)^{-1}\mathbf{Y}\mathbf{Y}'$. By definition of eigenvectors and eigenvalues, we have

$$\frac{1}{NT}\mathbf{Y}\mathbf{Y}'\tilde{\mathbf{F}} = \tilde{\mathbf{F}}V_{NT} \iff \frac{1}{NT}\mathbf{Y}\mathbf{Y}'\tilde{\mathbf{F}}V_{NT}^{-1} = \tilde{\mathbf{F}}, \quad (17)$$

where $\tilde{\mathbf{F}}'\tilde{\mathbf{F}} = \mathbb{I}_r$. The model defined in (1) and (2) can be re-written as

$$\begin{aligned} \mathbf{Y}_t &= [\mathbf{\Lambda}_0 + \mathbf{\Lambda}(t)]\mathbf{F}_t + \mathbf{e}_t \\ &= \mathbf{\Lambda}_0\mathbf{F}_t + \mathbf{\Lambda}(t)\mathbf{F}_t + \mathbf{e}_t \\ &= \mathbf{\Lambda}_0\mathbf{F}_t + \mathbf{w}_t + \mathbf{e}_t, \end{aligned}$$

where $\mathbf{w}_t = \mathbf{\Lambda}(t)\mathbf{F}_t$. Now, we define the following $T \times N$ matrices, $\mathbf{e} = (\mathbf{e}_1, \mathbf{e}_2, \dots, \mathbf{e}_T)'$ and $\mathbf{w} = (\mathbf{w}_1, \mathbf{w}_2, \dots, \mathbf{w}_T)'$. Note that the model in (1), can also be re-written in matrix form as

$$\mathbf{Y} = \mathbf{F}\mathbf{\Lambda}_0' + \mathbf{w} + \mathbf{e}.$$

Consequently, after taking products we get

$$\mathbf{Y}\mathbf{Y}' = \mathbf{F}\mathbf{\Lambda}_0'\mathbf{\Lambda}_0\mathbf{F}' + \mathbf{F}\mathbf{\Lambda}_0'(\mathbf{e} + \mathbf{w})' + (\mathbf{e} + \mathbf{w})\mathbf{\Lambda}_0\mathbf{F}' + (\mathbf{e} + \mathbf{w})(\mathbf{e} + \mathbf{w})'.$$

Then, from the definition of $\tilde{\mathbf{F}}_t$ in (17) and the matrix rotation H , we can write for a fixed t

$$\begin{aligned} \tilde{\mathbf{F}}_t - H'\mathbf{F}_t &= (NT)^{-1}V_{NT}^{-1}\tilde{\mathbf{F}}'\mathbf{Y}\mathbf{Y}'_t - V_{NT}^{-1}(\tilde{\mathbf{F}}'\mathbf{F}/T)(\mathbf{\Lambda}_0'\mathbf{\Lambda}_0/N)\mathbf{F}_t \\ &= \frac{V_{NT}^{-1}}{NT}[\tilde{\mathbf{F}}'(\mathbf{F}\mathbf{\Lambda}_0'\mathbf{\Lambda}_0\mathbf{F}_t + \mathbf{F}\mathbf{\Lambda}_0'(w_t + e_t) + (w_t + e_t)\mathbf{\Lambda}_0\mathbf{F}_t + (e_t + w_t)(e_t + w_t)) \\ &\quad - (\tilde{\mathbf{F}}'\mathbf{F})(\mathbf{\Lambda}_0'\mathbf{\Lambda}_0)\mathbf{F}_t] \\ &= \frac{V_{NT}^{-1}}{NT}[\underbrace{\tilde{\mathbf{F}}'\mathbf{F}\mathbf{\Lambda}_0'e_t}_{D_{1t}} + \underbrace{\tilde{\mathbf{F}}'e\mathbf{\Lambda}_0\mathbf{F}_t}_{D_{2t}} + \underbrace{\tilde{\mathbf{F}}'ee_t}_{D_{3t}} + \underbrace{\tilde{\mathbf{F}}'\mathbf{F}\mathbf{\Lambda}_0'w_t}_{D_{4t}} + \underbrace{\tilde{\mathbf{F}}'w\mathbf{\Lambda}_0\mathbf{F}_t}_{D_{5t}} + \underbrace{\tilde{\mathbf{F}}'ww_t}_{D_{6t}} + \\ &\quad \underbrace{\tilde{\mathbf{F}}'ew_t}_{D_{7t}} + \underbrace{\tilde{\mathbf{F}}'we_t}_{D_{8t}}] \\ &= V_{NT}^{-1}\sum_{i=1}^8 D_{it}. \end{aligned}$$

Then, after applying squared norms in both sides, adding on t , and dividing by T in $V_{NT}^{-1}\sum_{i=1}^8 D_{it}$, we get by the L $\tilde{\mathbf{A}}$ inequality

$$\frac{1}{T}\sum_{t=1}^T \|\tilde{\mathbf{F}}_t - H'\mathbf{F}_t\|^2 \leq \|V_{NT}^{-1}\|^2 8 \sum_{i=1}^8 \left(\frac{1}{T} \sum_{t=1}^T \|D_{it}\|^2 \right) \quad (18)$$

where

$$\begin{aligned}
D_{1t} &= \tilde{\mathbf{F}}' \mathbf{F} \mathbf{\Lambda}'_0 e_t / NT & D_{2t} &= \tilde{\mathbf{F}}' e \mathbf{\Lambda}_0 \mathbf{F}_t / NT \\
D_{3t} &= \tilde{\mathbf{F}}' e e_t / NT & D_{4t} &= \tilde{\mathbf{F}}' \mathbf{F} \mathbf{\Lambda}'_0 w_t / NT \\
D_{5t} &= \tilde{\mathbf{F}}' w \mathbf{\Lambda}_0 \mathbf{F}_t / NT & D_{6t} &= \tilde{\mathbf{F}}' w w_t / NT \\
D_{7t} &= \tilde{\mathbf{F}}' e w_t / NT & D_{8t} &= \tilde{\mathbf{F}}' w e_t / NT
\end{aligned}$$

Then, from [Mikkelsen et al. \(2018\)](#) (Lemma A.1), V_{NT} converges to a definite positive matrix, therefore $\|V_{NT}^{-1}\| = O_p(1)$. Considering Assumptions A-E and properties of principal components, for each term $D_{it}, i = 1, \dots, 8$, we have

$$\begin{aligned}
T^{-1} \sum_{t=1}^T \|D_{1t}\|^2 &= O_p(N^{-1}), \\
T^{-1} \sum_{t=1}^T \|D_{2t}\|^2 &= O_p(N^{-1}T^{-1}), \\
T^{-1} \sum_{t=1}^T \|D_{3t}\|^2 &= O_p(N^{-1}T^{-1}), \\
T^{-1} \sum_{t=1}^T \|D_{4t}\|^2 &= O_p(N^{-2}K_{1NT}), \\
T^{-1} \sum_{t=1}^T \|D_{5t}\|^2 &= O_p(N^{-2}T^{-2}K_{2NT}), \\
T^{-1} \sum_{t=1}^T \|D_{6t}\|^2 &= O_p(N^{-2}T^{-2}K_{3NT}), \\
T^{-1} \sum_{t=1}^T \|D_{7t}\|^2 &= O_p(N^{-2}K_{1NT}), \\
T^{-1} \sum_{t=1}^T \|D_{8t}\|^2 &= O_p(N^{-2}K_{1NT}).
\end{aligned}$$

Finally, the right-hand side of equation (18) is a sum of variables with orders $\left\{ \frac{1}{N}, \frac{1}{NT}, \frac{K_{1NT}}{N^2}, \frac{K_{2NT}}{N^2T^2}, \frac{K_{3NT}}{N^2T^2} \right\}$, respectively, and the proof is now completed. \square

B Figures for Section 4

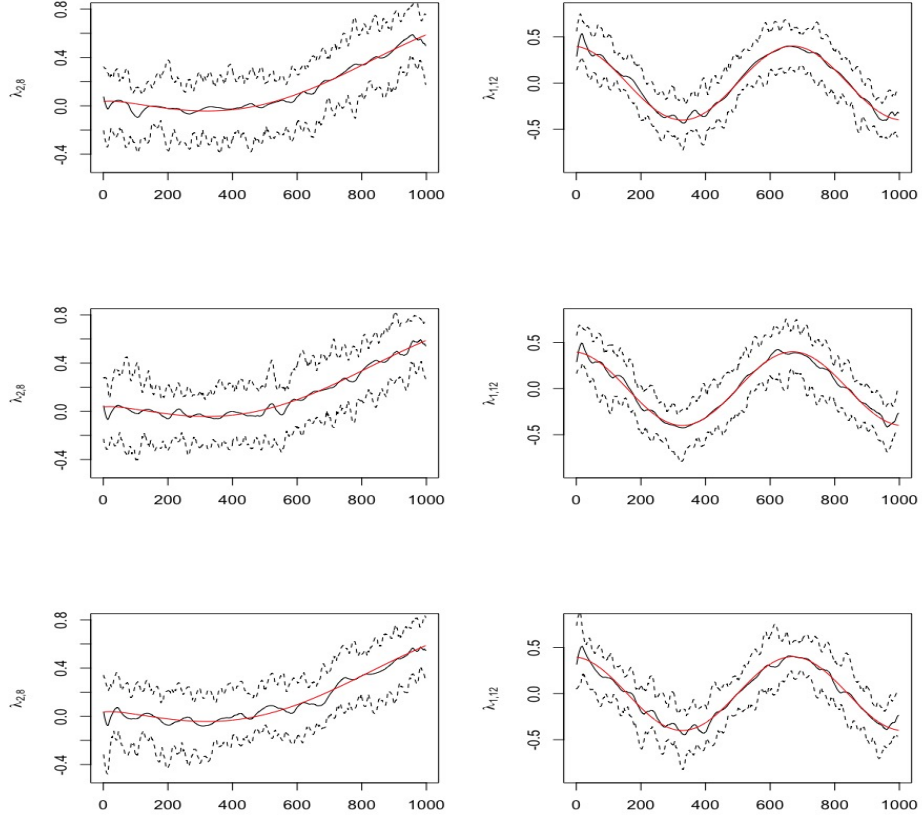


Figure 1: Comparison between the actual factor loadings (solid red line), the estimated factor loadings (solid black line), and Bootstrap confidence interval at 95% (dashed black line). By column, from left to right: $\lambda_{1,12}$, and $\lambda_{2,8}$. By row, from top to bottom: $\theta_k = 0$, $\theta_k = 0.5$, and $\theta_k = 1$, for $k \in \{1, 2\}$. $\Gamma_e = Toep$, $N = 20$, $T = 1024$ and Wavelet Haar.

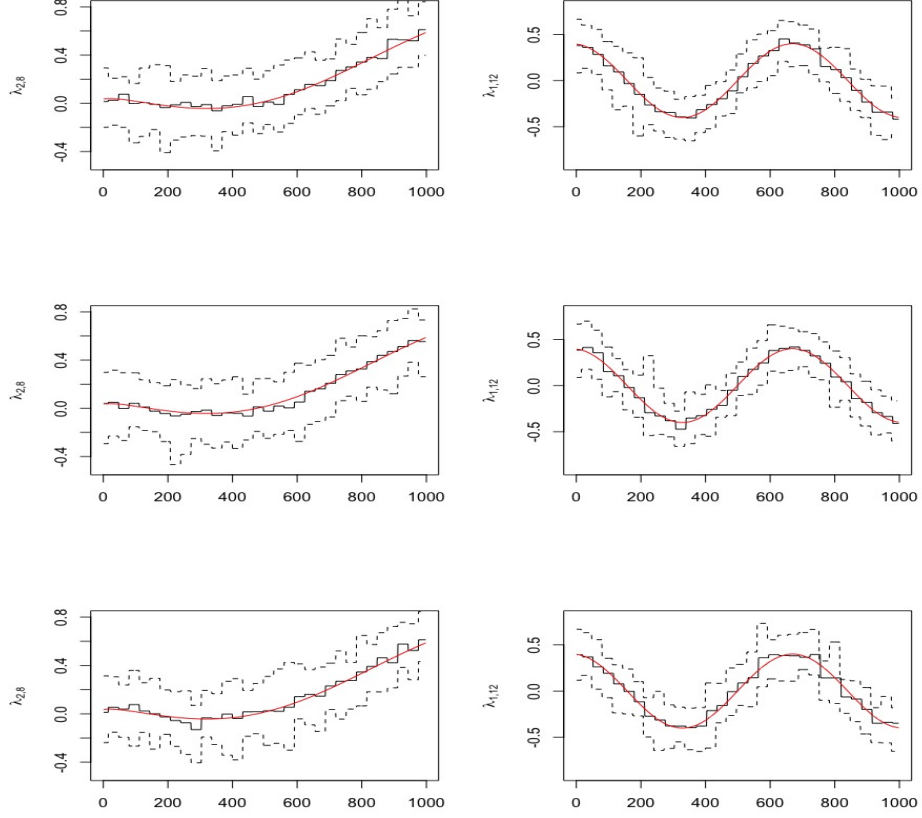


Figure 2: Comparison between the actual factor loadings (solid red line), the estimated factor loadings (solid black line), and Bootstrap confidence interval at 95% (dashed black line). By column, from left to right: $\lambda_{1,12}$, and $\lambda_{2,8}$. By row, from top to bottom: $\theta_k = 0$, $\theta_k = 0.5$, and $\theta_k = 1$, for $k \in \{1, 2\}$. $\Gamma_e = \text{Toep}$, $N = 20$, $T = 1024$ and Wavelet D8.